2021 5th International Conference on Electrical Engineering and Information & Communication Technology (ICEEICT)
Military Institute of Science and Technology (MIST), Dhaka-1216, Bangladesh

2021 5th International Conference on Electrical Engineering and Information & Communication Technology (ICEEICT) | 978-1-6654-9522-6/21/$31.00 ©2021 IEEE | DOI: 10.1109/ICEEICT53905.2021.9667897

PID, LQR, and LQG Controllers to Maintain the Stability of an AVR System at Varied Model Parameters

Md. Rayid Hasan Mojumder
Department of Electrical and Electronic Engineering
Khulna University of Engineering & Technology
Khulna 9203, Bangladesh
rayid.pf@gmail.com

Naruttam Kumar Roy
Department of Electrical and Electronic Engineering
Khulna University of Engineering & Technology
Khulna 9203, Bangladesh
nkroy@eee.kuet.ac.bd

***Abstract*—This research demonstrates the time-domain performance characteristics of proportional-integral-derivative (PID), linear quadratic regulator (LQR), and linear quadratic gaussian (LQG) controllers when the gain parameters and time constants of an automatic voltage regulator (AVR) system change. We tuned the amplifier and sensor block gains and scrutinized the change in the stability. Also, we investigated the system response while the time constant of the amplifier, exciter, generator, and sensor blocks are set to their maximum permissible limit. We determined the eigenvalues of the system and observed that the location of close loop poles is very much susceptive to time constant variations. The LQG controller provides a comparatively faster and stable response than LQR and PID. When the gain parameters and time constants of the static AVR system are varied, the PID performance decreases significantly, but LQR and LQG can track the change rapidly. This analysis indicates that the impact of plant parameters on the controller response will be crucial while implementing the dynamic power system with distributed generators and interconnected grids.**

Keywords—Automatic voltage regulator, Linear Quadratic Regulator, Linear-Quadratic Gaussian, Proportional Integral Derivative, Power system control, Step response

I. INTRODUCTION

In conventional power generating stations, especially of steam, hydro, gas, or combined-cycle power plants, a synchronous generator (SG) is used to generate electricity with the help of a turbine and speed governor. The SG generates a specified voltage value depending on the rotor excitation and the mechanical design of windings and poles. Any reactive power burden can alter the rated voltage output of the SG with higher line losses [1]. Moreover, the fluctuation of power line voltages affects the loads connected to the system. This generates significant instability to the power system and increases the maintenance and operating costs. To improve the system stability and maintain the generator's terminal voltage, an automatic voltage regulator (AVR) system is always used in today's power plants. During any contingency, if the terminal voltage of SG changes, AVR tunes the exciter output voltage of the SG and forces the terminal voltage to revert to the nominal voltage [2]. It is thus required that AVR should react in a fast and dynamic manner to reduce any induced voltage instability of the system. To improve the system dynamics of AVR, controllers such as proportional integral derivative (PID), Sugeno fuzzy logic (SFL), and model predictive controller (MPC) are often integrated into the system. PID-based robust controlling has garnered significant attention due to its structural simplicity and robustness of operation [3]. However, the parameters of PID gains are very much susceptible to non-linear and variable operating loads.

AVR system tunes the exciter voltage in a manner to offset the load variation on the SG terminal. The investigation of step response of a PID-based AVR system reveals that generally, the maximum peak overshoot with various optimization algorithms stays within 1.0 to 1.3 per unit (p.u.) value of the nominal terminal voltage [4]. The prevalent optimization algorithms provide a peak time of ~ 0.35 sec. Moreover, recently, the lowest rise time and settling time are achieved with a stochastic fractal search algorithm as 0.103 sec and 0.584 sec, respectively [5]. The performance of the PID-based optimization algorithms depends largely on the objective and cost functions used and differs from each other when a custom object function is proposed. Heuristical algorithms with computation burden are required to tune the PID gains for an efficient controller operation [6]. In recent years, however, modern controllers such as linear quadratic regulator (LQR), linear quadratic gaussian (LQG), and model predictive controller (MPC) are comprehensively applied in applications extending from power systems to aerospace to automatic vehicles [7]–[9]. System response could be improved in terms of robustness by substituting PID controllers with LQR or LQG.

In [10], an LQG-DC control scheme is proposed for an AVR system. A single area grid isolated power system is considered to investigate the improvement of the overshoot damping efficiency of the AVR system. The resultant system response is then compared with PID, LQR, and LQG controllers to outline the efficacy of the proposed LQG-DC system. In [11], a hybrid AC/DC microgrid is considered to analyze the damping and tracking control of the subgrid voltage through implementing an integral-LQG controller. Various undefined loads are considered during the investigation that causes the voltage fluctuation of the subgrid system model. The authors summarized that the proposed controller enhances the robustness of the system. In load flow control (LFC) of the power system, LQR and LQG are extensively used. It is addressed that the intrinsic settling time of 8 sec of an LFC system can be reduced to less than 5 sec with the help of an LQR controller [10]. In LQR, the unique minima of the quadratic cost function are enumerated by solving the algebraic Riccati equation in linear system dynamics. The design parameters, Q and R, penalize the state variables and control signals, respectively. Choosing a large value of R and a small value of Q matrix correspondingly results in an expensive control strategy and greater change in

978-1-6654-9522-6/21/$31.00 ©2021 IEEE

system states. In a system where large controller signals can result in the saturation of the actuator or increases system noise, the value of the R matrix is kept limited. A trade-off between the Q and R is often considered by using trial and error methods. In case of LQG, a Gaussian noise and a state estimator (Kalman filter) is additionally added to the LQR system since the system state may not be directly observable due to the random variables and noises.

From the above literature, it is clear that the transient response of an AVR system needs to be improved to alleviate any voltage variation introduced due to no-load, half load, disturbances, or faults within a permissible limit. It is also required that the controller used for such an operation be robust, fast, and structurally considerably simple. Due to changes in system operating conditions, often, the gain parameters and time constants of the generator, amplifier, and sensors used in the AVR system, are altered from their set values. In the current literature, comprehensive analysis of different novel controller models and control theories are being proposed and existent, but a majority of those investigation focuses on the AVR dynamics in connection with power grid dynamics. The investigation of the AVR system parameters' (gains and time constants) sensitivity in the absence of grid and/or load dynamics is lacking. This constrains the prediction of the AVR blocks sensitivities when it is embedded within a complex dynamic power system modeling since, while doing so, prior information regarding the controller response at altered AVR system parameters is crucial, especially with PID controller implementation. Thus, herein we designed and considered a grid-isolated AVR system with PID, LQR, and LQG controllers and observed the effect and sensitivities of the subsystems gain parameters and time constants variation on the terminal voltage output via analyzing step (0 to 1) controller input response. In a systematic way, we delineated a comparative study of the PID, LQR, and LQG systems by forcing the AVR subsystem block parameters at their maximum and minimum values. In a grid-isolated AVR system, we observed that gain parameters and time constants affect significantly and the sensitivity of these parameters behave differently with PID, LQR, and LQG controllers. Among the three controllers, PID shows the highest susceptibility to parameter variations. A state estimator to the LQR system could enhance system response during any gain parameter, time constant, and voltage step variation. Our investigation reveals that the LQG controller works better to control the AVR system of an SG than the LQR and PID system.

The rest of the paper is arranged in the following manner: in Section II, modeling of the AVR system is discussed; Section III summarizes the mathematical design of the PID, LQR, and LQG controllers for the AVR system. AVR system implemented with the proposed dynamic PID, LQR, and LQG controllers is then analyzed in Section IV. The comparative investigation of the AVR step response with various parameter variations is attached in Section V. Finally, Section VI concludes the paper.

II. AVR SYSTEM MODEL

An AVR system improves the power system voltage stability by employing the excitation control. The generator's terminal voltage is kept in the vicinity of the nominal voltage by the AVR system at different operating conditions. In an economical way, the field exciter is operated to retain the generator's output voltage to the desired value. The entire AVR system comprises four basic subsystems: amplifier, exciter, generator, and sensor. For the sake of control system analysis, the saturation and non-linearity are dropped from the subsystem's transfer function. At the same time, the gain parameters and time constant of the specific block are considered explicitly. Fig. 1 describes the AVR subsystems, where $V_{ref}(s)$, $V_s(s)$, $E(s)$, $V_R(s)$, $V_F(s)$, and $V_T(s)$ are the reference voltage, sensor output voltage, error signal, exciter input voltage, field excitation voltage, and generator terminal voltage. The closed-loop transfer function for the AVR system becomes:

$$G_{AVR}(s) = \frac{V_T(s)}{V_{ref}(s)} = \frac{K_A K_E K_G (1+T_S s)}{(1+T_A s)(1+T_E s)(1+T_G s)(1+T_s s)+K_A K_E K_G K_S} \quad (1)$$

The standard range of the gain parameters and time constants for the isolated system and the value considered herein to model the AVR system is mentioned in TABLE I. The step response of the considered AVR system demonstrates very poor time-domain characteristics. From Fig. 2, the rise time, settling time, steady-state error, and others could be perceived. As can be seen, an effective additional controller arrangement is required to make the AVR system more robust and stable to retain system voltage under different system parameters variations.

III. CONTROLLER DESIGN

In this section, the design and mathematical relations pertaining to the PID, LQR, and LQG controllers are detailed. These controllers are embedded in the considered AVR system. We observed the AVR system response with these controllers while varying the time constant and gain parameter of the AVR subsystems.

A. Design of PID controller

The PID controller uses the proportional-integral-derivate components to reduce the error between the actual setpoint for the system parameter and the current parameter value.

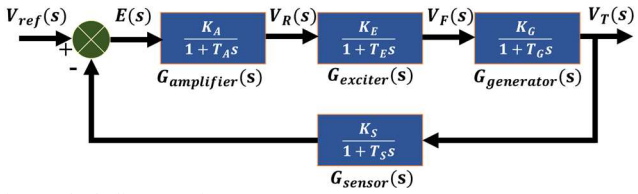

Fig. 1. Block diagram of an AVR system.

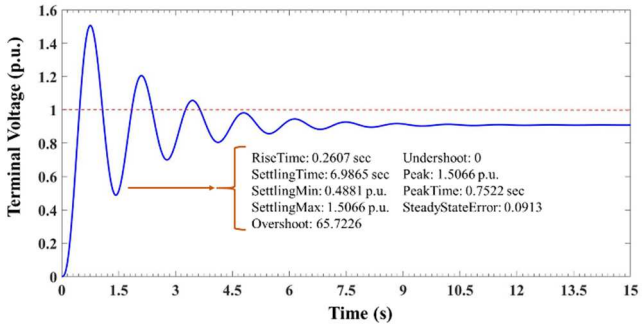

Fig. 2. Terminal voltage variation of an AVR system.

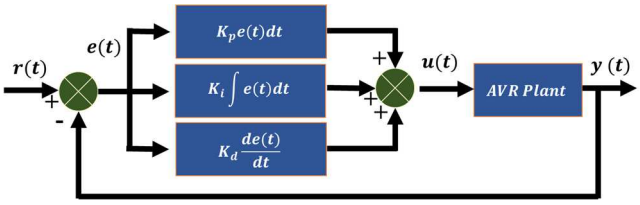

Fig. 3. Block diagram of a PID feedback controller.

Considering Fig. 3, $r(t)$ being the reference set point and $y(t)$ the measurand system parameters, PID controller utilizes the error signal, $e(t) = r(t) - y(t)$And dispatches correction measures to reduce the value of $e(t)$ over time. A controlled variable $u(t)$ is updated to a new value coming from a weighted combination of the P-I-D variables is employed in this regard to reduce the error signal. Mathematically the PID controller control function could be expressed as:

$$u(t) = K_p e(t) + K_i \int_0^T e(t)dt + K_d \frac{de(t)}{dt} \quad (2)$$

TABLE I. TIME CONSTANT AND GAIN PARAMETER VALUES FOR AN AVR SYSTEM.

	Gain parameter	*The time constant (s)*	*Value considered*
Amplifier	$10 \le K_A \le 40$	$0.02 \le T_A \le 0.1$	$K_A = 10$, $T_A = 0.1$ s
Exciter	$1.0 \le K_E \le 10$	$0.5 \le T_E \le 1.0$	$K_E = 1.0$, $T_E = 0.5$ s
Generator	$0.7 \le K_G \le 1.0$	$1.0 \le T_G \le 2.0$	$K_G = 1.0$, $T_G = 1.0$ s
Sensor	$1.0 \le K_S \le 2.0$	$0.001 \le T_S \le 0.06$	$K_S = 1.0$, $T_S = 0.01$ s

Where K_p , K_i , and K_d refers to the non-zero gain parameters for the proportional, integral, and derivative units. The proportional (P) unit responses focusing whether the error at present is large or small and positive or negative and takes a value proportionately to minimize the error. In the absence of error, unit P is zero. The integral (I) part cumulates the past values of the error signal by integrating errors over time and works to minimize the residual error value after the proportional control is dispatched. The derivate (D) unit predicts the future trends of the error signal focusing on the current rate of change of error signal $e(r)$. Being a derivate term of the error, a higher rate of error signal change will call upon more damping control.

In this research, we considered the Ziegler–Nichols (ZN) tuning method to tune the K_p, K_i, and K_d parameter values. We set the parameters at $Kp = 0.4755$, $Ki = 0.90057$, and $Kd = 0.06277$. The performance (time of response, bandwidth) and robustness (static or dynamic) are set as the criteria to determine the desired parameters. A large K_p value results in a higher rise time but increased overshoot. The K_i parameter reduces steady-state error but increases the settling time between the desired and actual process output values. Increased K_d value reduces the overshoot and settling time of the system. The type of controller (P, PI, or PID) to be used and the algorithms or process to tune the gain parameter value often depends on the application and the plant where the controller system is operated.

B. Design of LQR controller

The LQR controller is an optimal control regulator system that enhances the system dynamics by employing a feedback gain. It aims to obtain a proper control law to minimize a quadratic objective function. The plant is described as follow:

$$\frac{dx(t)}{dt} = Ax(t) + Bu(t) \quad (3)$$

$$y(t) = Cx(t) + Du(t) \quad (4)$$

Where, $\frac{dx(t)}{dt}$, $u(t)$, and $y(t)$ are the derivative of the state vector, input vector, and output vector, respectively while maintaining range, $x(t) \in R^n$, $u(t) \in R^p$, and $y(t) \in R^m$. Here, A is the state matrix of order $n \times n$, B is the input matrix of order $n \times p$, C is the output matrix of order $q \times n$, and D is the feedforward matrix of order $q \times p$. When the system contains no feedforward value, this matrix is set at zero. The quadric objective function for LQR is:

$$J = \int_0^\infty (x(t)Qx(t) + u^T(t)Ru(t))dt \quad (5)$$

Here, the R ($R = R^T$) and Q matrices are called the positive control weighting matrix and non-negative state weighting matrix, respectively. When a larger value of R is selected, it will penalize the control signal, and the control strategy becomes expensive. A larger value of Q will impose a small possible change on the state variables to minimizes the above cost function. Using the algebraic Riccati equation (ARE), the unique minimum of the cost function could be determined. A trade-off between the Q and R-value is often considered to create a robust optimal control system with feasible controller complexity and expense. The Block diagram of the LQR control model is shown in Fig. 4.

The state feedback method, $u(t) = -Kx(t)$, is used to obtain the optimal position of the cost function (J). K is the controller gain and depends on the positive and unique solution (P) of the ARE:

$$K = R^{-1}B^T P \quad (6)$$

$$A^T P + PA - PBR^{-1}B^T P + Q = 0 \quad (7)$$

C. Design of LQG controller

The LQG controller makes use of LQR with an additional state estimator, the Kalman estimator. It can be used in both linear time-invariant and variant systems and can deal with uncertain system disturbances, such as Gaussian white noise. In LQG, the system's process noise and measurement noise are added to the system block to present a robust system.

The state feedback law of LQR can not directly be used here due to additional noises added to the state variable, making state information incomplete at the summation node of the control loop. The Kalman filter takes the distorted state variables as the input, utilizes in-built optimal recursive data processing procedures, and provides a precise value of the state of interest. The goal is to decrease the tracking error between the command signal and controller output value measured. Fig. 5 represents the simplified block diagram of the LQG controller. The state-space representation of a linearized plant model with added Gaussian noises and the corresponding quadratic cost function can be represented as:

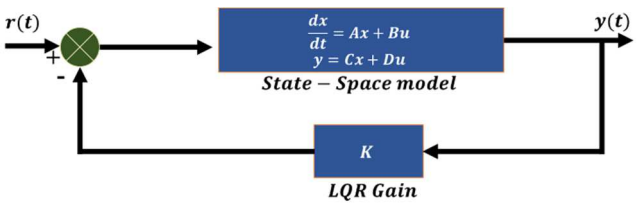

Fig. 4. Block diagram of an LQR feedback controller.

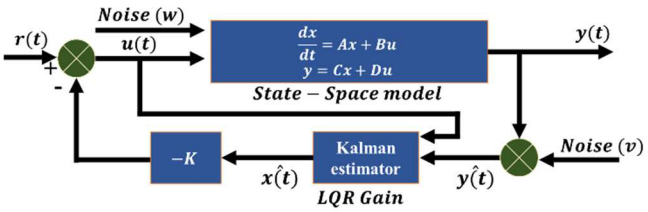

Fig. 5. Block diagram of an LQG feedback controller.

$$\frac{dx(t)}{dt} = Ax(t) + Bu(t) + D_1 w_{pn} \quad (8)$$

$$y(t) = Cx(t) + Du(t) + D_2 w_{mn} \quad (9)$$

$$J = \lim_{T\to+\infty} E\frac{1}{T}\int_0^T (x(t)Qx(t) + u^T(t)Ru(t))dt \quad (10)$$

The variables A, B, C, D, $x(t)$, $u(t)$, and $y(t)$ refer to the same as for the LQR model. D_1 and D_2 refers to the noise matrices of the system. Additional, w_{pn} and w_{mn} denotes the Gaussian process noise and Gaussian measurement noise, respectively. E refers to the expected value. The LQG controller with Kalman state observer is defined as:

$$\dot{\hat{x}}(t) = A\hat{x}(t) + Bu(t) + K_k\big(y(t) - \hat{y}(t)\big) \quad (11)$$

$$u(t) = -L\hat{x}(t) \quad (12)$$

where, $\hat{x}(t)$ and $\hat{y}(t)$ are the estimated value of the state vector, $x(t)$, and output vector, $y(t)$. The physically non-measurable states are converted to the required feedback states at the output of the Kalman filter, which depends on the observer gain matrix, L. K_k is the Kalman gain. The detailed Kalman observe design and the associated recursive data processing steps are delineated in [12].

IV. Performance of AVR System without a Controller

This section discusses the observed characteristics of an AVR system without any controller. The AVR plant is designed by considering the generator, sensor, amplifier, and exciter time constants and gain parameters as demonstrated in TABLE I. The step response of the AVR system (Fig. 1.) shows oscillatory nature, and the response comes along a large settling time. This can be explained via observing the closed-loop poles and zeros location on the root locus plot given in Fig. 6(a). The underdamped response mostly results due to the pole pair in the close vicinity of the imaginary axis line. Two of the close-loop poles are very near to the positive x-axis.

The poor stability of the system can also be perceived by analyzing the bode diagram (Fig. 6(b)). The phase cross-over frequency (4.4050 rads^{-1}) for the AVR system is lesser than the gain cross-over frequency (6.1238 rads^{-1}). Moreover, both the gain margin (GM) and phase margin (PM) are narrow for the system. We calculated the GM and PM using the following relations to be 1.9250 dB and 18.593°, respectively:

$$GM = 20\log\left(\frac{1}{M_{pc}}\right) dB = -20\log(M_{pc})\ dB \quad (13)$$

$$PM = 180° + \varphi_{pc} \quad (14)$$

Where, M_{pc} is the gain magnitude at the phase cross-over frequency and φ_{pc} is the phase angle at the gain cross-over frequency.

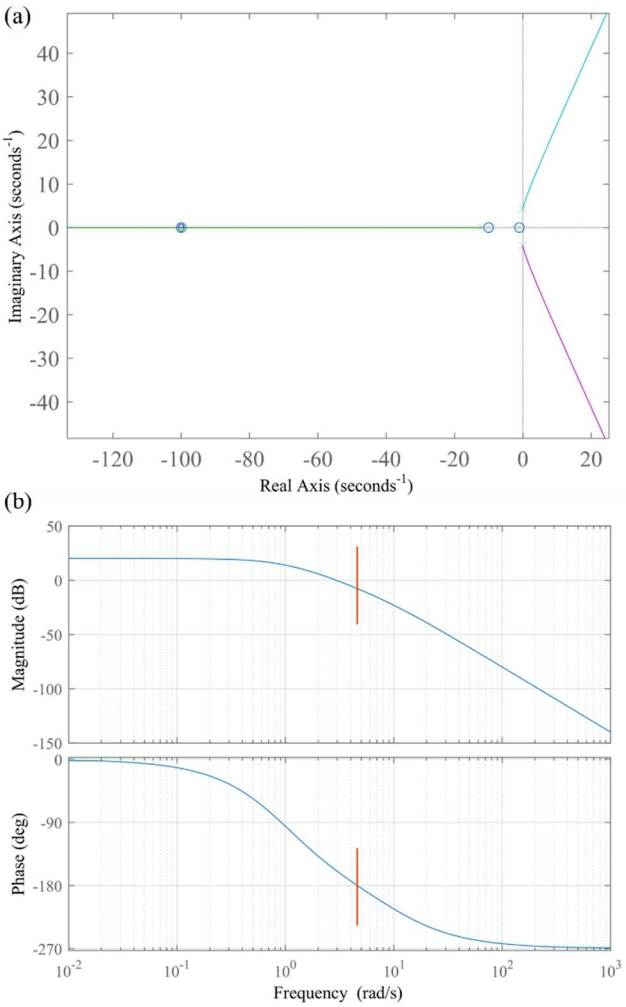

Fig. 6. (a) Closed-loop root-locus plot of AVR system without controller. (a) Root locus plot and (b) Bode diagram of an open-loop AVR system.

V. Comparative Analysis of the Controllers

To further investigate and scrutinize the benefit of using any particular controller discussed here for the AVR system, in this part, we provide some comparative studies. TABLE II represents the closed-loop poles for the AVR system with our considered controllers. The pair of complex poles residing very close to the imaginary axis line is mitigated by embedding the controllers. The poles of LQR are on a far negative side than the LQR and PID, thus will enhance system stability. The number of closed-loop poles decreases for the LQR and LQG systems.

The step response and associated terminal voltage controlling for PID, LQR, and LQG controllers are depicted in Fig. 7. It can be observed that the response with the PID controller requires quite a higher settling period than the rest two. In TABLE III, we summarized the peak time, rise time, settling time, overshoot, and steady-state error parameters for each of the controllers. The lowest steady-state error is obtained with the LQG controller to be ~ 0.0000064% and the highest steady-state error result with PID controller ~ 0.015%. Also, the overshoot with the PID controller is much higher than LQR. The LQG controller provides the lowest rise time,

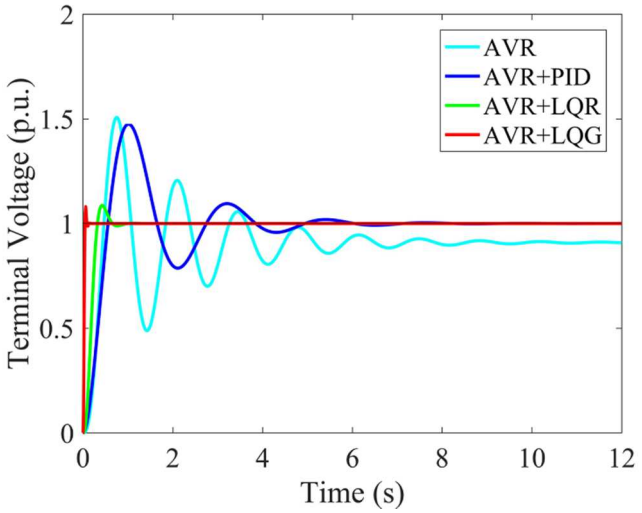

Fig. 7. The step response and associated terminal voltage controlling for PID, LQR, and LQG controllers.

settling time, and steady-state error, while the time to reach the peak closely matches the time obtained with the LQR controller. We figured that the trial-and-error manual controlling of the controller parameters and the minimization of the cost function with advanced optimization techniques could be increased significantly. It is to be noted that the control weighting matrix, R, is heavily weighted in the LQG system to design a very fast system.

TABLE II. LOCATION OF CLOSED-LOOP POLES OF AVR SYSTEM WITH DIFFERENT CONTROLLER ARRANGEMENTS.

Without controller	*PID controller*	*LQR controller*	*LQG controller*
-99.9 + 0.0i	-0.5 + 0.0i	-99.9 + 0.0i	-59.5 + 102.8i
-12.4 + 0.0i	-100.1 + 0.0i	-19.5 + 0.0i	-59.5 – 102.8i
-10.0 + 0.0i	-10.0 + 0.0i	-8.62 +14.2i	-118.9 + 0.0i
-0.52 + 4.7i	-4.59+ 4.95i	-8.62 -14.2i	-100.1 + 0.0i
-0.52 - 4.7i	-4.59 – 4.95i	-10.0 + 0.00i	-10.0 + 0.0i
-2.5+ 0.0i	-2.71 + 0.0i	-2.5 + 0.00i	-2.50 + 0.0i
-1.0 + 0.0i	-2.50 + 0.0i	-1.0 + 0.00i	-1.00 + 0.0i
	-1.09 + 0.0i		
	-1.00 + 0.0i		

TABLE III. TIME DOMAIN CHARACTERISTICS OF AN AVR SYSTEM WITH PID, LQR, AND LQG CONTROLLERS.

	Without Controller	*PID*	*LQR*	*LQG*
Rise Time (s)	0.2607	0.3841	0.1979	0.0282
Settling Time (s)	6.9865	4.7135	0.5974	0.0809
Peak Time (s)	1.5066	1.0016	0.4293	0.0611
Peak (p. u.)	0.7522	1.4744	1.0864	1.0805
Overshoot (%)	65.7226	47.4385	8.6426	8.0523
Steady state Error (%)	9.18	0.014809	0.000015	0.0000064

Then keeping the subsystems gain parameter unaltered, we maximized the time constants and observed the step output (Fig. 8). The step response becomes too poor for the PID, followed by the LQR system. The PID parameter provides an undamped oscillation, and the system is totally unstable. This is because of increased time constant shift closed-loop system (with PID) poles to the right half plan of the s-plane. It is required either to use the ZN method to tune PID parameters to this new system constraints or to employ heuristical optimization algorithms to automatically update the PID gain based on the variation in system parameters or disturbance.

When the sensor feedback gain is increased, there appears a distinct stability concern for the PID controller (Fig. 9). The PID provides a very poor response since the parameters were tuned by the ZN method for a lower sensor gain value. Both the LQR and LQG system reverts the output value to the desired value in a fast manner. In Fig. 10, we exclusively tuned the amplifier gain value from 10 to 40 in a step size of 10 and the response of each controller separately. Higher amplifier gain results in a higher magnification of error of the system; thus, the controllers operating characteristics improved. For all the three considered controllers, the highest amplifier gain ($Ka = 40$) results in the lowest rise time and settling time. However, the gain can not be increased by more than 40 since that will represent an impractical AVR design.

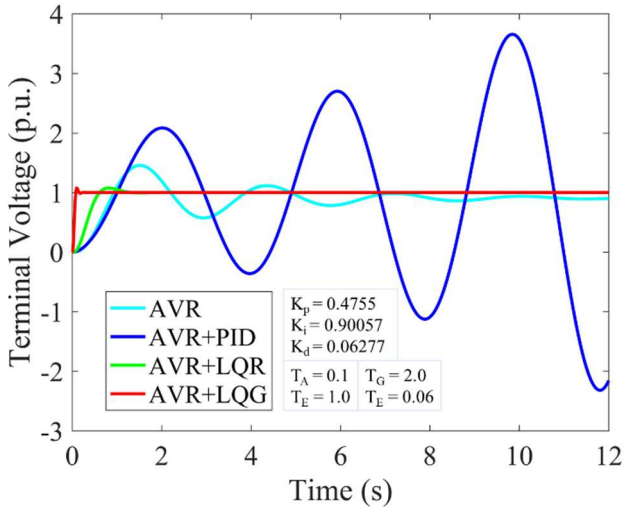

Fig. 8. The step response and associated terminal voltage controlling for PID, LQR, and LQG controllers when time constant for AVR subsystems are kept maximum.

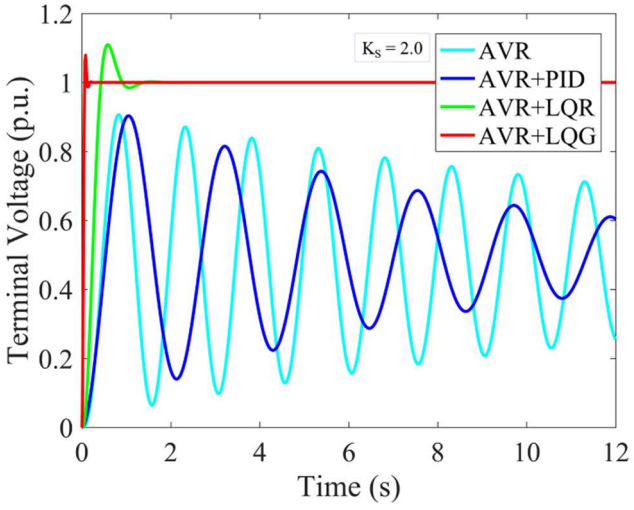

Fig. 9. The step response and associated terminal voltage controlling for PID, LQR, and LQG controllers. Sensor gain is set at 2.0.

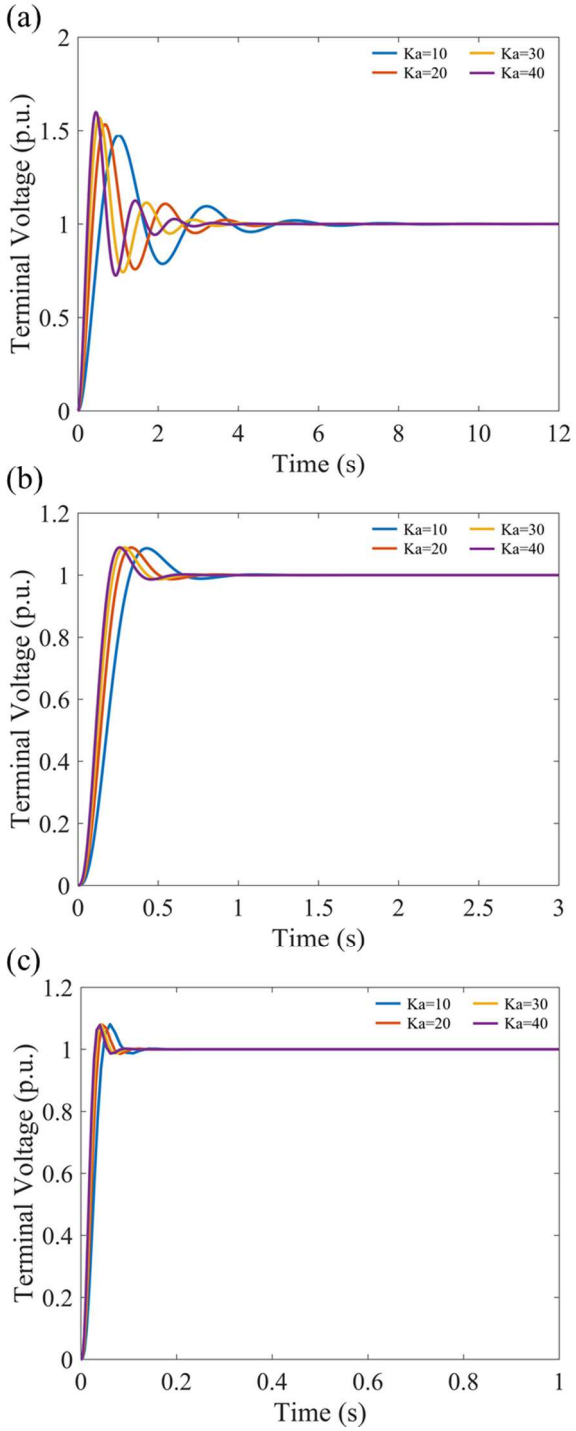

Fig. 10. The step response and associated terminal voltage controlling for (a) PID, (b) LQR, and (c) LQG, when amplifier gain is varied from 10 to 40.

VI. Conclusion

In this investigation, we have designed and analyzed the dynamic behaviors of a grid isolated automatic voltage regulator system at various subsystem gain parameters and time constant values. Moreover, we depicted how these system parameters variation affect differently with PID, LQR, and LQG controllers while reverting the generator terminal voltage to the nominal voltage in case of any input variation. We also summarized the comparative time-domain characteristics of these controllers for the AVR system. We obtained that the LQG controller block provides the fastest response with the lowest rise time, settling time, and steady-state error. The performance of LQR seconds the LQG in terms of a fast response. PID controller is very much subjected to gain parameter or time constant variations and needs separate tuning or optimization when system constrain change. This investigation sheds light on what to expect while implementing PID, LQR, and LQG in a dynamic power system and how the variations in the plant parameters alter the controller outputs. In the future, the performance of these controllers could be investigated for renewable-based distributed generator units.

References

[1] G. Fusco and M. Russo, 'Adaptive Voltage Regulator Design for Synchronous Generator', *IEEE Transactions on Energy Conversion*, vol. 23, no. 3, pp. 946–956, Sep. 2008, doi: 10.1109/TEC.2008.921463.

[2] A. J. H. Al Gizi, 'A particle swarm optimization, fuzzy PID controller with generator automatic voltage regulator', *Soft Comput*, vol. 23, no. 18, Art. no. 18, Sep. 2019, doi: 10.1007/s00500-018-3483-4.

[3] K. J. Åström and T. Hägglund, 'The future of PID control', *Control Engineering Practice*, vol. 9, no. 11, Art. no. 11, Nov. 2001, doi: 10.1016/S0967-0661(01)00062-4.

[4] H. Gozde and M. C. Taplamacioglu, 'Comparative performance analysis of artificial bee colony algorithm for automatic voltage regulator (AVR) system', *Journal of the Franklin Institute*, vol. 348, no. 8, Art. no. 8, Oct. 2011, doi: 10.1016/j.jfranklin.2011.05.012.

[5] E. Çelik, 'Incorporation of stochastic fractal search algorithm into efficient design of PID controller for an automatic voltage regulator system', *Neural Comput & Applic*, vol. 30, no. 6, Art. no. 6, Sep. 2018, doi: 10.1007/s00521-017-3335-7.

[6] S. Ekinci and B. Hekimoğlu, 'Improved Kidney-Inspired Algorithm Approach for Tuning of PID Controller in AVR System', *IEEE Access*, vol. 7, pp. 39935–39947, 2019, doi: 10.1109/ACCESS.2019.2906980.

[7] R. Panigrahi, B. Subudhi, and P. C. Panda, 'A Robust LQG Servo Control Strategy of Shunt-Active Power Filter for Power Quality Enhancement', *IEEE Transactions on Power Electronics*, vol. 31, no. 4, pp. 2860–2869, Apr. 2016, doi: 10.1109/TPEL.2015.2456155.

[8] 'A Multiobjective MPC Approach for Autonomously Driven Electric Vehicles', *IFAC-PapersOnLine*, vol. 50, no. 1, pp. 8674–8679, Jul. 2017, doi: 10.1016/j.ifacol.2017.08.1526.

[9] X. Liu, Q. Sun, and J. E. Cooper, 'LQG based model predictive control for gust load alleviation', *Aerospace Science and Technology*, vol. 71, pp. 499–509, Dec. 2017, doi: 10.1016/j.ast.2017.10.006.

[10] F. Tabassum and M. S. Rana, 'An Optimal LQG-DC Control for Compensating Voltage Fluctuation in a Single Area Power System', in *2019 International Conference on Computer, Communication, Chemical, Materials and Electronic Engineering (IC4ME2)*, Jul. 2019, pp. 1–4. doi: 10.1109/IC4ME247184.2019.9036552.

[11] S. K. Das, D. Datta, SubrataK. Sarker, S. R. Fahim, Md. R. Islam Sheikh, and F. R. Badal, 'Improved Voltage Oscillation Damping and Tracking of Subgrid of a Hybrid AC/DC Microgrid using Robust Integral Linear Quadratic Gaussian Control', in *2020 2nd International Conference on Smart Power Internet Energy Systems (SPIES)*, Sep. 2020, pp. 299–304. doi: 10.1109/SPIES48661.2020.9242969.

[12] M. Rahman, S. K. Sarkar, S. K. Das, and Y. Miao, 'A comparative study of LQR, LQG, and integral LQG controller for frequency control of interconnected smart grid', in *2017 3rd International Conference on Electrical Information and Communication Technology (EICT)*, Dec. 2017, pp. 1–6. doi: 10.1109/EICT.2017.8275216.